J Electr Eng Technol Vol. 8, No. 4: 911-919, 2013
http://dx.doi.org/10.5370/JEET.2013.8.4.911

ISSN(Print) 1975-0102
ISSN(Online) 2093-7423

Advanced LDC Test Bed Using Energy Recovery Technique for HEVs

Yun-Sung Kim*, Dong-Wook Jung and Byoung-Kuk Lee†**

Abstract – This paper reports the development of test bed with the energy recovering technique using two-step boost converter. The device is utilized for LDC aging test of Hyundai Motor's LPI AVANTE HEV in mass production. The developed power recycle type test bed is designed as 1.5 kW class to test up to the maximum load power of LDC and is also designed to supply scant power supply up to 500 W after power recycle. The theoretical design analysis and operational characteristics analysis results of test bed are reported, and its practicality and reliability are verified through the test result. Also, the finally developed test bed confirms approximately 79~85 % energy saving effect compared to the usual traditional aging test system.

Keywords: Boost converter, Eco-friendly electric vehicles, Energy recovery, Forward converter, Hybrid electric vehicles, Low DC-DC converter, Phase shift full bridge converter

1. Introduction

DC-DC converters used in eco-friendly electric vehicles such as Hybrid Electric Vehicles (HEVs) and Electric Vehicles (EVs) needs the high reliability than the existing converter for industrial and home use. Especially, the high reliability from the production stage is required for low DC-DC converter (LDC) because LDC belongs to driving system. In general aging tests of LDCs, external input power is required, and output power is lost as heat through the load device. Accordingly, solutions to reduce input power installation cost and get rid of load heat consumption during aging tests are required. This study introduces a way to reuse the input of LDC by recycling output power. The proposed power recycling structure is an energy cyclic structure, as show in Fig. 1(b). Meanwhile, Fig. 1(a) is a common test environment, and it consists of the input power supply device and output load resistor or output electronic load. At that time, all of output load capacity and LDC losses should supply from input power supply device and they are burned as heat from load device.

The developed test bed activates LDC by setting the input at low capacity after the initial startup. The low-level output voltage of an LDC is used as an input source of the test device. The developed test bed supplies this voltage again to the LDC by boosting it up to the LDC input level. At this time, LDC loss energy is compensated by additionally using external power. Therefore, the demand energy for LDC aging is saved as much as the sum of loss energy form the LDC and that form the test device. This paper explains the operation characteristics of configuration circuit and the running sequence of test bed. Also, the great of the proposed method is verified by measuring the saved power compared to the traditional system through the actual aging test.

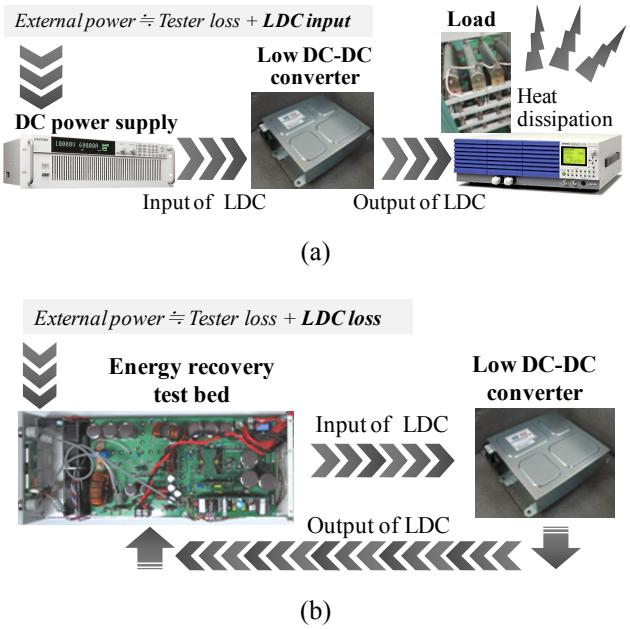

Fig. 1. Concept diagram of energy recovery test bed: (a) General aging test bed; (b) Proposed aging test bed.

2. Design Consideration for LDC Test Bed

2.1 Characteristics and role of LDC

LDC uses power of the high voltage battery saving

† Corresponding Author: College of Information & Communication Engineering, SungKyunKwan University, Korea. (bkleeskku@skku.edu)
* College of Information & Communication Engineering, SungKyunKwan University, Korea. (yunsk@skku.edu)
** Research & Development Center, Dongah Elecomm Co., Ltd, Korea. (dwjung@dongahelecomm.co.kr)
Received: May 27, 2013; Accepted: June 7, 2013

driving energy. LDC is supplied with high voltage from batteries of 130~400 V_{DC}, and control and output various voltages within approximately a 12~15 V_{DC} range if the level is set to 12 V_{DC}. In the development case of this study, the output power of the LDC is 1.5 kW class, the rated input voltage is 180 V_{DC}, and the rated output voltage is 13.9 V_{DC}. As shown in Fig. 2, the negative pole on the primarily side of LDC is connected to the negative pole of a high-voltage battery. The negative pole on the secondary side is connected to the negative pole of a low-voltage battery and the vehicle frame. LDC is designed as an isolated topology. EMI filter structure is simple because LDC performs DC-to-DC power conversion, and full-bridge types are mainly used to meet high efficiency performance requirements [1-4].

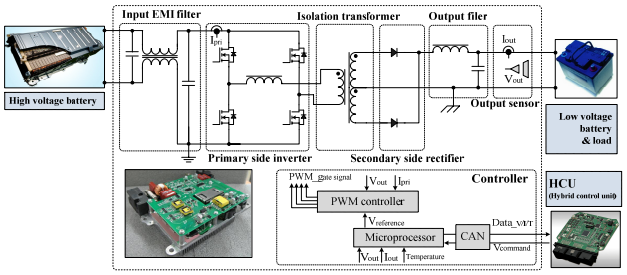

Fig. 2. Composition of LDC.

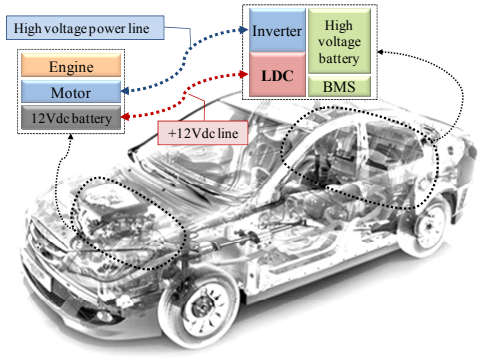

(a)

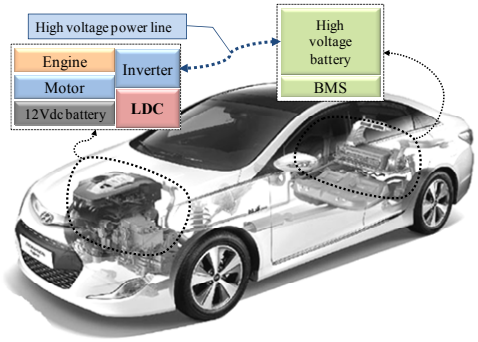

(b)

Fig. 3. LDC mounting structure inside HEVs: (a) Truck room mounting structure; (b) Engine room mounting structure.

The general characteristics of LDCs are as follows: 1) It requires more than 90 % of high efficiencies in most operation section; 2) The input and the output voltages are variable. Power with high density is required; 3) Long term operational durability characteristics are needed; 4) The improvement topology of half bridge and full bridge, forward mainly applied and it communicates with upper device by using DSP or microprocessor.

Fig. 3(a) is a vehicle installation case of a truck room mounted LDC. In this case, the LDC module is a stand-alone forced air type, and an HEV from Honda Motor Co., Ltd is represented. Fig. 3(b) shows the installation case of an engine room mounted LDC. An HEV from TOYOTA Motor Co., Ltd is represented, and the LDC has inverter and HDC integral water cooling system structure. Test bed of this research is developed to target at trunk room-mount LDC but it can be applied to LDC of engine room-mount type.

2.2 Design conditions of test bed

Test bed should have conditions considering operation characteristics of LDC. First, they judge whether voltage of the output low voltage battery is normal or not before starting up. At that time, an inner auxiliary power stage works by using high-voltage battery power on the input side for basic communication with the upper controller. If there is problem with voltage supply on the input side, communication is maintained by using low-voltage battery power on the output side, and the problem is conveyed to the upper controller. After confirming that the voltage on the input and output side is normal, LDC receives a starting command from the upper controller and starts operation.

The input voltage supply and voltage generator device that play the role of a low-voltage battery within a normal voltage range are required for LDC startup. An LDC is designed as an isolated topology, but a separate isolation specification is not required in aging testing environments. Therefore, non-isolated circuit structure design is also possible. The circuit structure of energy cycle type test beds has advantages, in that non-isolated topology can achieve relatively high efficiency compared with isolated topology and the circuit is simple. However, if the input-output step down ratio is high, non-isolated topology can work with theoretical step up ratio because of duty losses and sensitivity of control by parasitic elements of the circuit. Also, power losses in LDCs should be compensated for externally since the output power of the LDC is used again as input power.

In this paper, a two-step boost converter (Hereafter TS-Boost converter) is applied to resolve the limits of non-isolated topology, and higher output voltage gain than general boost converter is implemented. Also, in order to compensate for the lack of power, a two-transistor forward converter (Hereafter TT-Forward converter), which is a simple design and is easy control, is applied to the

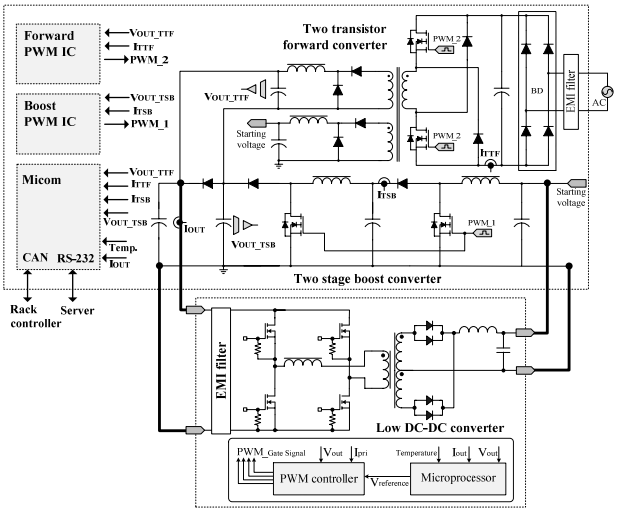

Fig. 4. Basic circuit diagram of test bed and wiring structure.

topology over medium capacity. Meanwhile, the supply of external power supply is designed so as not to influence LDC operation. Like in Fig. 4, the test bed consists of a recycling, which receives output power from the LDC and converts it to input power, and an isolated circuit stage, which compensates for the losses of LDC. The power loss of the TS-Boost converter becomes the output load capacity of the TT-Forward converter, and the entire power requirement is the sum of the power loss in the TS-Boost converter and the power loss in TT-Forward converter [5-10].

$$P_{LDC\_input} = P_{LDC\_output} + P_{LDC\_loss} \quad (1)$$

$$P_{Test\ Bed\_input} \fallingdotseq P_{LDC\_loss} + P_{Test\ Bed\_loss} \quad (2)$$

$$P_{Test\ Bed\_loss} = P_{TS-Boost\_loss} + P_{TT-Forward\_loss} \quad (3)$$

2.3 Analysis of TT-Forward converter

Generally, forward topology is widely applied to medium, small capacity power conversion. Especially, unlike single transistor forward converters, TT-Forward converter has the advantage that FET voltage stress is the same as the input voltage, making FET applications with relatively low voltage specifications is possible. Generally, with a smaller voltage specification of FET, one can expect efficiency improvement since R_{DS} can be reduced. The TT-Forward converter circuit structure can be implemented simply through a simple serial FET addition on the transformer primary wire. Two FETs turn on/off via the same gate signal. Accumulated transformer magnetizing energy in the on section is reset via two clamping diodes in the off section. That is, self clamping for the magnetizing current reset of the power transformer is possible without a complicated reset circuit. A rectifier stage on the secondary side is the same as basic forward converter.

Fig. 5 shows the operation mode depending on the

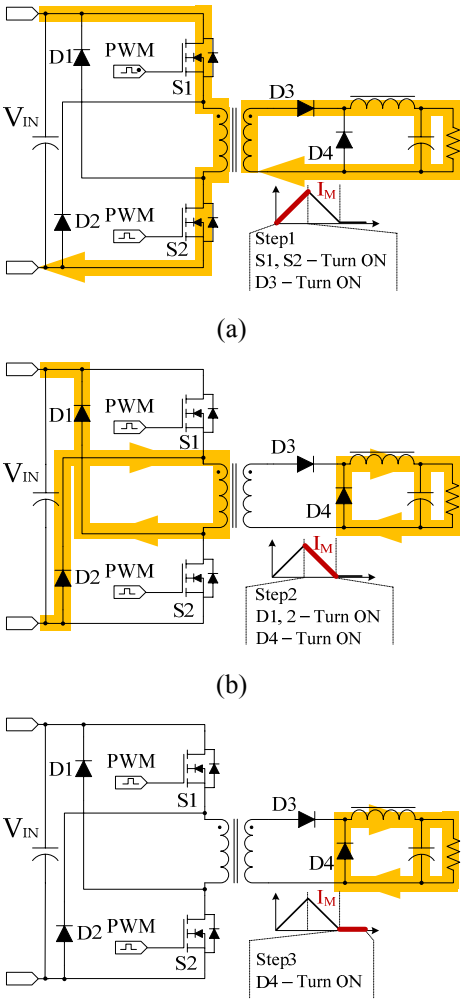

Fig. 5. Operation mode of TT-Forward converter: (a) FET turn-on mode; (b) Diode turn-on mode; (c) Idle mode.

switching of the TT-Forward converter. Relations between the input and output of the TT-Forward converter and turn ratio of the transformer inductance are as follows [11, 12].

$$V_{OUT} = \eta \cdot V_{IN\_min} \cdot D_{max} \cdot N \quad (4)$$

$$N = \frac{V_{OUT}}{\eta \cdot V_{IN\_min} \cdot D_{max}} \quad (5)$$

$$L_{mag} = \frac{V_{in\_min} \cdot D_{max}}{(0.1 \cdot I_{P-PK}) \cdot f_{sw}} \quad (6)$$

Here, V_{IN_min} is the input minimum voltage, D_{max} is the maximum duty ratio and N is the turn ratio. L_{mag} is the primary side inductance, and $(0.1 \times I_{P\text{-}Pk})$ is the 10 % ratio of primary side current.

2.4 Analysis of TS-Boost converter

Two FETs of the TS-Boost converter designed in this paper are controlled at the same time. The operating

characteristic of the TS-Boost converter in normal state is shown in Fig. 6. The output voltage gain characteristic of the TS-Boost converter is unlike that of general single boost converters. Eqs. (7)-(10) are the relations between the TS-Boost converter input and output voltages depending on the current mode of Boost1 and Boost2. Fig. 7 represents the results of Eqs. (7)~(10) when the input voltage is 12 V_{DC} and switching frequency is 40 kHz. In the test bed, the main operating voltage section of the TS-Boost converter is about 120 V_{DC}, and the current mode of each stage can boost up the output voltage in the duty range of 0.6~0.7% regardless of CCM or DCM. The maximum sizes of output voltage and duty range are estimated through Fig. 7. The CCM-DCM combination is best suited for obtaining wide output voltage gain. Meanwhile, the CCM-CCM combination is superior for controlling stability. DCM-DCM and DCM-CCM have similar output voltage gain characteristics. The actual output voltage is measured and compared by duty in the open loop state of the test bed in the graph. The analysis result of CCM-CCM mode until 0.6 % is measured with the same output voltage. It is changed to CCM-DCM mode at duty 0.7 %. In the main output voltage range of the test

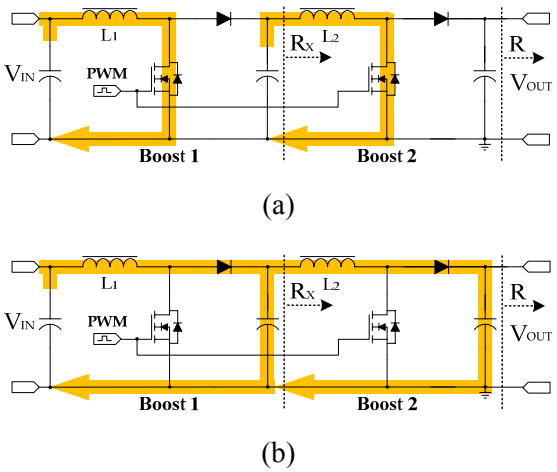

Fig. 6. Operation of TS-Boost converter: (a) FET turn-on mode; (b) Diode turn-on mode.

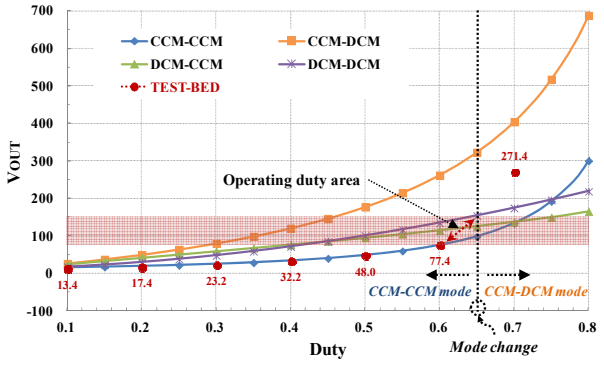

Fig. 7. V_{OUT} by each current mode and actual duty ratio, V_{IN}=12 V_{DC}, F_{SW}= 40 kHz.

bed, two modes are operated mainly on the changed boundary [13-15].

$$V_O = \frac{V_{IN}}{(1-D)^2} \text{ [CCM-CCM]} \tag{7}$$

$$V_O = \frac{1}{2} \cdot \frac{1}{(1-D)} \cdot \left(1 + \sqrt{1 + \frac{2 \cdot D^2 \cdot R \cdot T_s}{L_2}}\right) \cdot V_{IN} \text{ [CCM-DCM]} \tag{8}$$

$$V_O = \frac{1}{2} \cdot \frac{1}{(1-D)} \cdot \left(1 + \sqrt{1 + \frac{2 \cdot D^2 \cdot (1-D)^2 \cdot R \cdot T_s}{L_1}}\right) \cdot V_{IN} \text{ [DCM-CCM]} \tag{9}$$

$$V_O = \frac{1}{4}\left(1 + \sqrt{1 + \frac{2 \cdot D^2 \cdot R_X T_s}{L_1}}\right)\left(1 + \sqrt{1 + \frac{2 \cdot D^2 \cdot R \cdot T_s}{L_2}}\right) V_{IN} \text{ [DCM-DCM]} \tag{10}$$

$$R_x = \frac{R}{\left(1 + \sqrt{1 + \frac{2 \cdot D^2 \cdot R \cdot T_S}{L_2}}\right)^2} \tag{11}$$

Here, R is the final equivalent resistance, R_x is the equivalent resistance of Boost1 and Ts is the cycle. L_1 is the inductance of Boost1, and L_2 is the inductance of Boost2.

2.5 Operation mode and sequence analysis of test bed

Fig. 8 is the power flow by operating mode of the test bed. If the system power supply is inserted in Fig. 8(a), the TT-Forward converter begins to start up. The TT-Forward converter outputs the main output voltage of 60 V_{DC} and the sub output voltage of 12 V_{DC}. At this time, the auxiliary output of 12 V_{DC} is approved for input of the TS-Boost converter and the LDC output side. The sub output of 12 V_{DC} approved for the TS-Boost converter in Fig. 8(b) is boosted up to 120 V_{DC}. At this time, the series combination output stage of the TS-Boost converter and the TT-Forward converter is boosted up to a total of 180 V_{DC}.

Output voltage combined in series begins LDC operation from range exceeding input under voltage point of LDC before recycle mode starts like Fig. 8(c). From this point, power does not supply the sub output voltage of 12 V_{DC} because the LDC output voltage is higher than the sub output voltage of the TT-Forward converter. Fig. 8(c) is the full-scale recycle operating mode, and the normal state is operated by adjusting the amount of LDC output load through constant current control of the TS-Boost converter. Fig. 9 is the operating sequence chart of the test bed. The start time of each item can be changed through an inner microprocessor, and the time at the bottom of the chart in Fig. 9 is the application time of the actual prototype.

2.6. Analysis of simulation operation mode

Using PSIM simulation, power supply flow of each

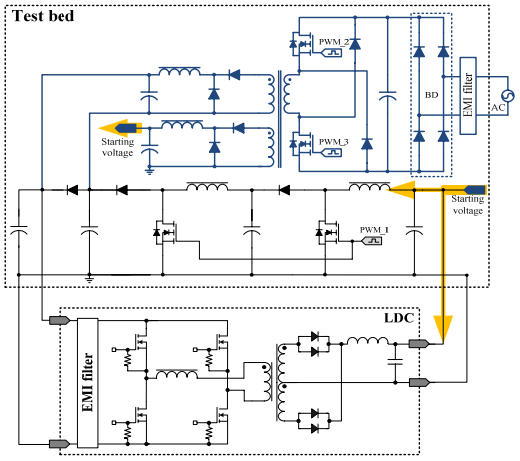

(a)

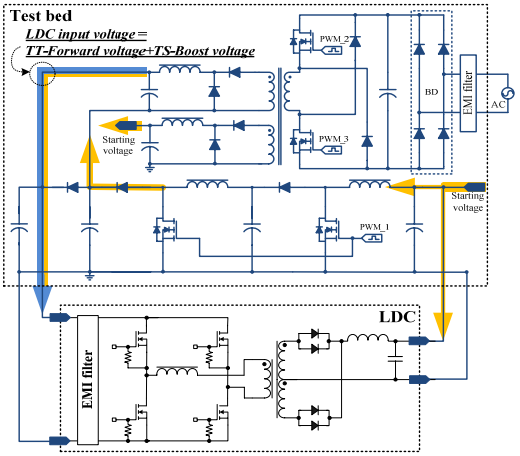

(b)

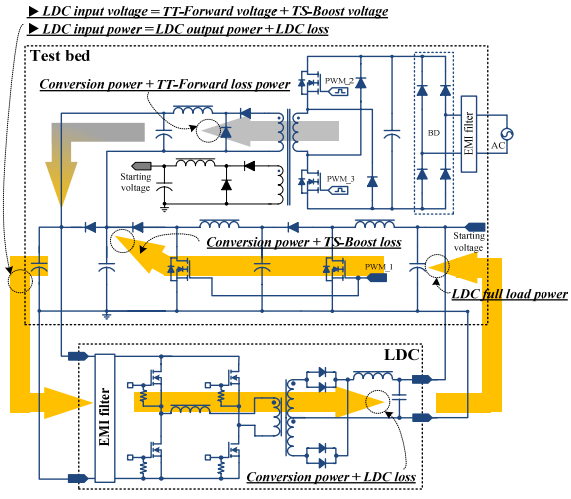

(c)

Fig. 8. Operation mode of test bed: (a) TT-Forward converter operating start, approvement on starting voltage to LDC; (b) TS-Boost converter operating start, high voltage output of TS-Boost converter; (c) Recycle operating start, normal operation of LDC.

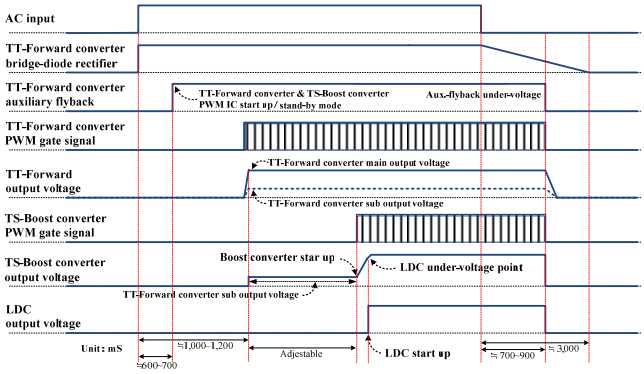

Fig. 9. Operation sequence of each test bed stage.

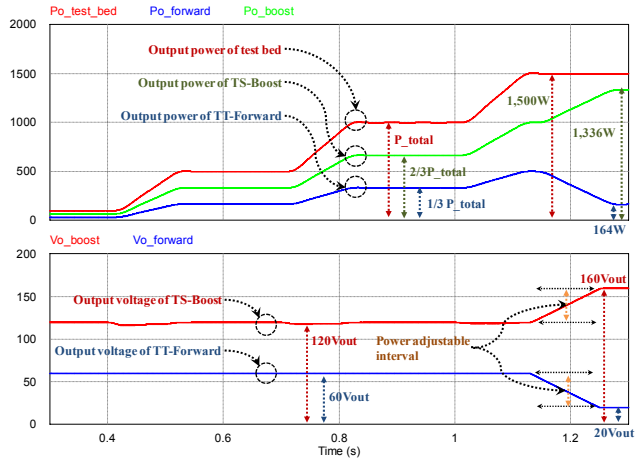

Fig. 10. Result of simulation operation mode.

stage is confirmed. Fig. 10 shows share ratio the output power of TT-Forward converter and TS-Boost converter when output power of test bed increases. The output power steps up to 500 W, 1,000 W, and 1,500 W, distribution power for each state can be checked. In comparison with the total of output power $P_{\_total}$ for each segment, the TS-Boost converter distributes output power of two thirds and the TT-Forward converter distributes output power of one thirds. At this point, the TS-Boost converter is controlled by output voltage 120 V_{DC}. The TT-Forward converter is controlled by output voltage 60 V_{DC}. In other words, share ratio of power is controlled by the output voltage size of each stage.

And in more than 1,500 W, the TS-boost converter is controlled for rising output voltage in order to recycle as much as possible the supplied power from LDC. On the other hand the output voltage of TT-forward converter is controlled for falling into the same as the voltage rising of TS-Boost converter. Finally, the TS-Boost converter condition is eight times larger if being the TS-Boost converter to 160 V_{DC}, the TT-Forward converter to 20 V_{DC}.

Therefore, share distribution ratio of each output power at this time can be confirmed to be same proportion as 1,336 W, and 154 W. That is to say that test bed enhances energy recycling performance by controlling the output

voltage of TS-Boost converter in rated output section of LDC after setting output voltage control of each stage as a fixed value in transient load condition. Because setting a goal of fixed output with rated capacity of LDC, actual test bed can simply achieve a goal performance through voltage variable control of the TS-Boost converter.

3. Experimental Results of Test Bed

For the performance verification and characteristic analysis of the developed test bed, it is tested at the maximum output load conditions of LDC, and the effects on the power recycling are confirmed. The characteristics of the circuit are analyzed by measuring the operation waveforms. Fig. 11 is the internal structure of the test bed used in the test. The cooling method is forced air, and modification of the control through volume in the front is possible, as well as control through communication. Also, this paper reports about the power conversion module of the test bed, but each module is integrally controlled through a test rack system. The state of each LDC and test bed can be monitored and saved. Fig. 12 is a test waveform of operating sequence characteristics. Fig. 12(a) is the waveform until output voltage startup of TT-Forward converter after applying AC input. Fig. 12(b) is the discharge off characteristics of Boost1 and Boost2 after PWM of the TS-Boost converter is stopped by a control command. The discharge time of Boost1 is longer than that of Boost2 because of the link capacitor volume between Boost1 and Boost2.

Fig 12(c) is the results of measuring the surrounding current of the series couple diode on the final output side of the test bed. Fig. 13 shows the result of measuring the efficiency of each stage during the LDC load recycle operation. Error exists because measurements were taken in the combining state of the whole test bed. However, the efficiency aspects of each stage are confirmed. Also when the total load power of LDC is about 1.5 kW, the output power of the TT-Forward converter is 404 W, and the output power of the TS-Boost converter is 1,147 W. The TT-Forward converter compensates for the power loss of the LDC and the TS-Boost converter.

Figs. 14 and 15 show the measurement results of the

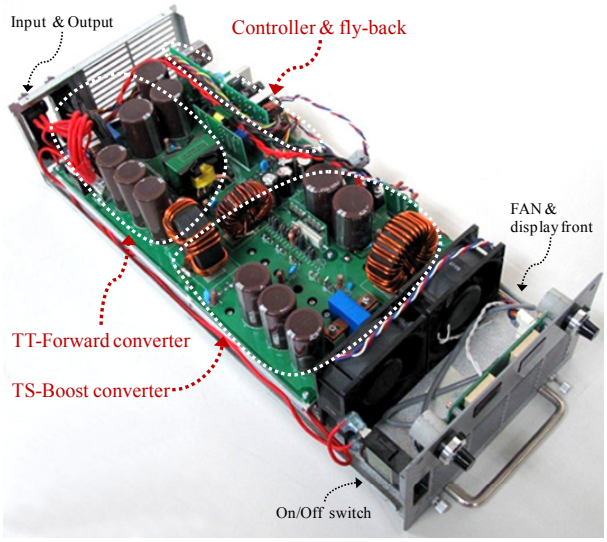

Fig. 11. Internal arrangement and external structure of test bed.

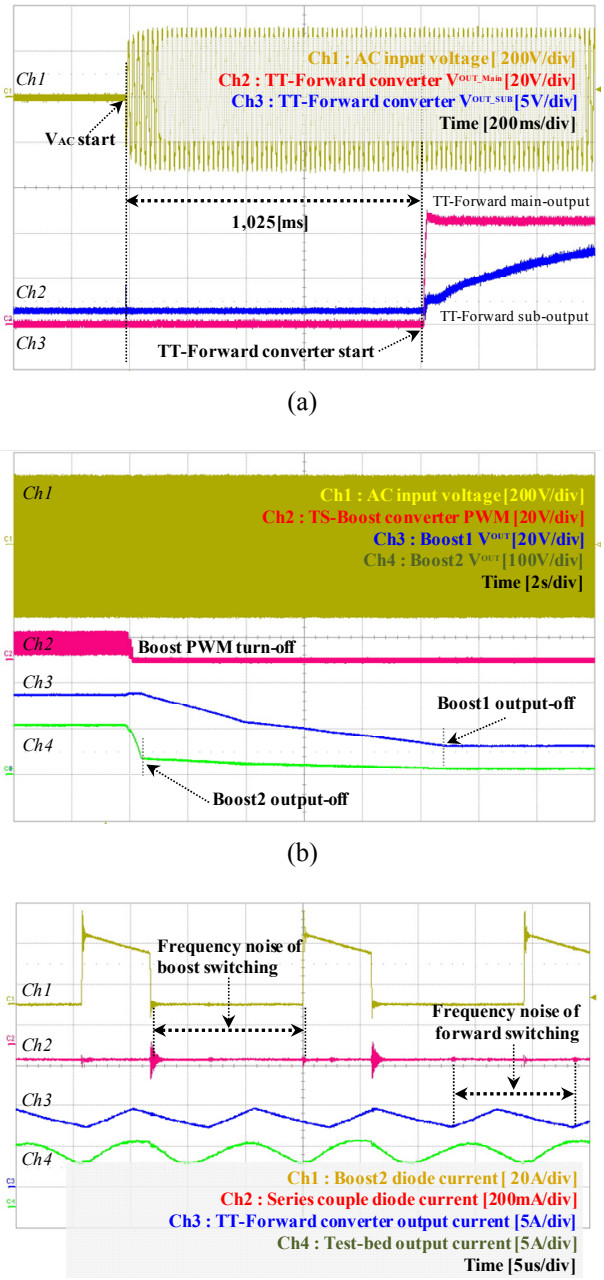

Fig. 12. Operation waveform result of test bed: (a) Turn-on test bed, starting waveform of test bed; (b) Turn-off test bed, off waveform of test bed; (c) Output side, current waveform of each stage.

amount of circulation power for confirming the power recycling effects of amount test bed. The graph in Fig. 14 is the result of measuring the input power when increasing the output load of the LDC by 10 % using the test bed. The test output power is the amount of output load power of the LDC, and input power is the external power supplied to the test bed through TT-Forward converter. The remaining power deducted input power from the test output power is recycled through the TS-Boost converter. 1,044 W can be recycled when testing at 1,500 W. Fig. 15 presents the final effects of the test bed with respect to the amount of power. The DC Source and DC Load in Fig. 15 mean consumption the power of each device if testing an LDC with the aging method using a general external device. The sum of the consumption power of the input and output devices are presented as the Total Power Used. A total of 2,258 W is needed for each piece of equipment if the testing output load of the LDC is about 1,510 W like in Fig. 14. About

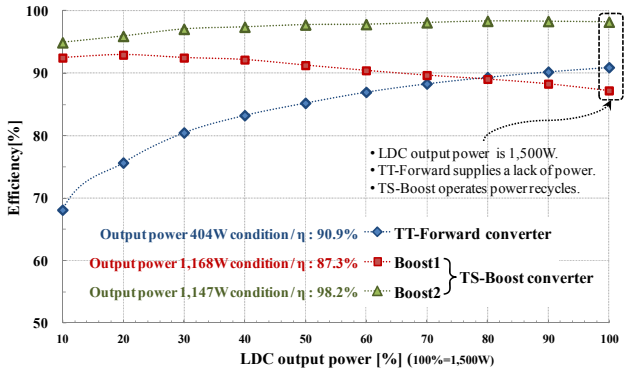

Fig. 13. Efficiency result of each stage by LDC load power.

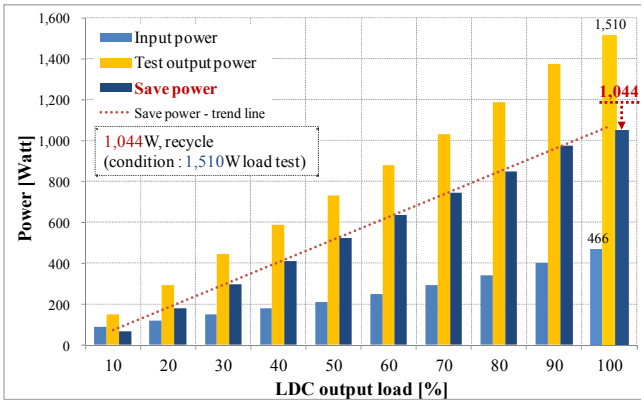

Fig. 14. Saving power result of power recycles.

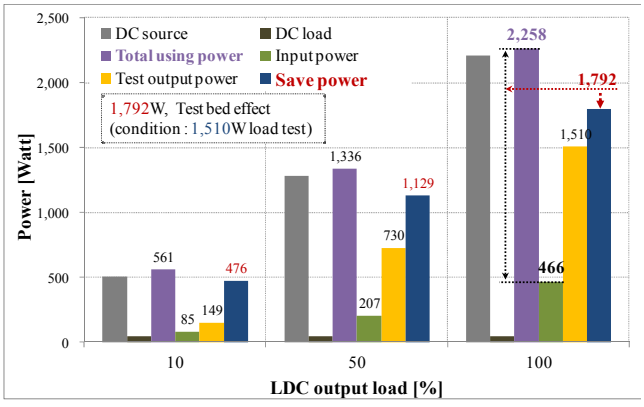

Fig. 15. Power saving effect of test bed.

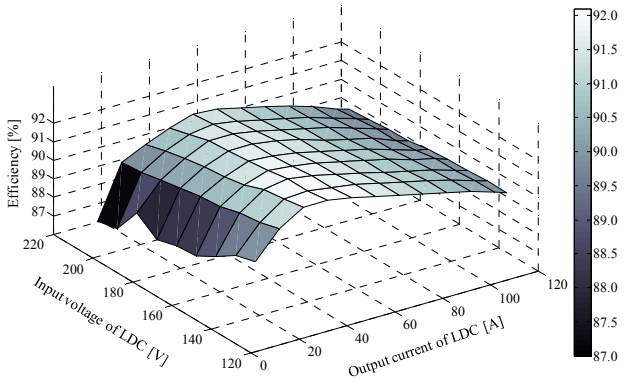

(a)

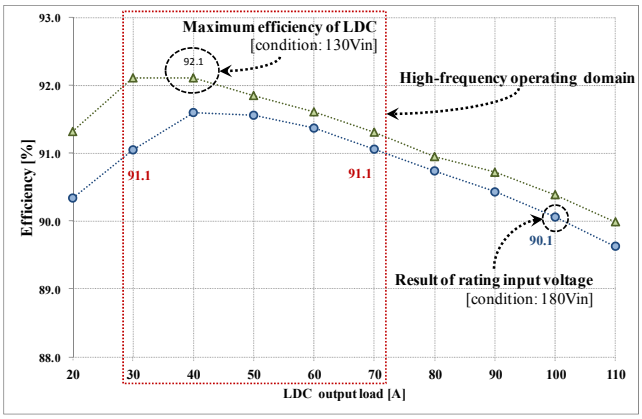

(b)

Fig. 16. Operating area efficiency distribution of LDC for HEV: (a) Efficiency distribution of whole operating area; (b) Rating input operating efficiency performance power.

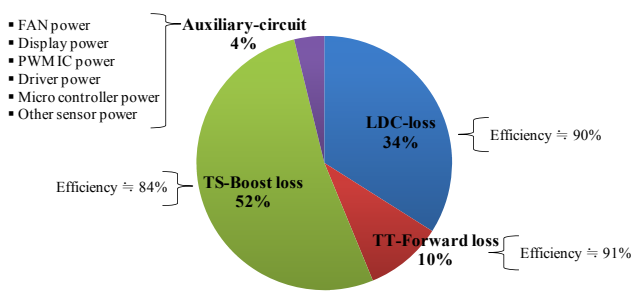

Fig. 17. Loss composition of test bed, 1,500 W load test.

700 W is generated by the LDC power loss and power loss of the device. The input power is reduced to 466 W when using the recycling test bed. The final power reduction effect of 1,792 W was measured. However, the quantitative numerical value can produce differences depending on the efficiency performance of the measurement device. For testing of Fig. 1, a SORENSE's SGI 600/25 model is used as the DC source, and a KIKUSUI's PLZ1003WH is used as the DC load. All power and efficiency measurements are taken using a YOKOGAWA's WT1600.

Figs. 16 and 17 is the graphs for analyzing 466 W additional power organization supplied to TT-Forward converter when testing 1,500 W load using test bed. Fig. 16 is the completed LDC efficiency performance for HEV. Fig. 16(a) is the efficiency distribution according to all load segments in the input entire section. Operation area of test bed is same as the rating operation range of LDC so, rating input voltage efficiency of LDC in Fig. 16(b) is important. Especially when testing 1,500 W load, about 90 % efficiency performances appear. Therefore, purely consumed loss distribution in LDC can be founded when test bed is working. Next, use distribution of additionally supplied power like Fig. 17 can be checked on reference efficiencies of each test bed stage in Fig. 13. In 466 W, loss of LDC is 34 %, one of TS-Boost converter is 52 %, one of TT-Forward converter is 10 %, and power consumption of fly-back circuit loss for internal auxiliary power and FAN, extra measurement and drive circuit account for 4 %. It can be found that actually consumed power in test bed is about 307 W.

4. Conclusion

This paper proposes LDCs aging test bed using energy recovery technique. Two-step boost converter with high step-up is applied for main power conversion of the proposed system and two-transistor forward converter is applied for auxiliary power compensation.

The operating characteristics of the TT-Forward converter were applied to the test bed and reviewed, and the output voltage gain characteristics of the TS-Boost converter were analyzed. The operating sequence of the test bed suited for LDCs tests was also designed. Electrical characteristics tests and performance tests were conducted using the produced prototype. As a result, the power recycling performance of 1,044 W was confirmed when testing a 1,500 W load of on the LDC. And the required total power confirms the energy saving effect of 1,792 W compared to the traditional system when testing 1,500 W, and running power ratio of test bed at that time can be seen as 66 %.

Furthermore, the structure of the introduced testing device can be applied through circuit modification for prototypes with various input and output specifications, as well as LDCs. In particular, a greater effect on cost reduction can be expected when producing high-capacity power supply devices. In particular, if being applied to large capacity power supply and battery charging and discharging system, large cost reduction effect can be expected.

References

[1] J. A. Sabate, V. Vlatkovic, R. B. Ridley, F. C. Lee, B. H. Cho, "Design considerations for high-voltage high-power full-bridge zero-voltage-switched PWM converter," APEC1990, pp. 275-284.

[2] L. H. Mweene, C. A. Wright, M. F. Schlecht, "A 1kW 500kHz front-end converter for a distributed power supply system," IEEE Transactions on Power Electronic, Vol. 6, No. 3, pp. 398-407, Jul. 1991.

[3] R. Redl, N. O. Sokal, L. Balogh, "A novel soft-switching full-bridge DC/DC converter: Analysis, design considerations, and experimental results at 1.5kW, 100kHz," PESC1990, pp. 162-172.

[4] Wu Chen, X. Ruan, R. Zhang, "A Novel Zero-Voltage-Switching PWM Full Bridge Converter," IEEE Transactions on Power Electronics, Vol. 23, No. 2, Mar. 2008, pp. 793-801.

[5] B.-R. Lin, K. Huang, D. Wang, "Analysis and implementation of full-bridge converter with current doubler rectifier," IEE Proceedings, Electric Power Applications, Vol. 152, No. 5, pp. 1193-1202, Sept. 2005.

[6] SongTingTing, HuangNianci, "A Novel Zero-Voltage and Zero-Current-Switching Full-Bridge PWM Converter," APEC 2003, Vol. 2, pp. 1088-1092.

[7] Xinbo Ruan, Yangguang Ya, "A Novel Zero-Voltage and Zero-Current-Switching PWM Full-Bridge Converter Using Two Diodes in Series With the Lagging Leg," IEEE Transactions on Industrial Electronics, Vol. 48, No. 4, pp. 777-785, Aug. 2001.

[8] Chris Iannello, Shiguo Luo, Issa Batarseh, "Full Bridge ZCS PWM Converter for High-Voltage High-Power Applications," IEEE Transactions on Aerospace and Electronics Systems, Vol. 38, No. 2, pp. 515-526, Apr. 2002.

[9] Yungtaek Jang, Milan M. Jovanovic, Yu-Ming Chang, "A New ZVS-PWM Full-Bridge Converter," IEEE Transactions on Power Electronics, Vol. 18, No. 5, pp. 1122-1129, Sept. 2003.

[10] Yungtaek Jang, Milan M. Jovanovic, "A New Family of Full-Bridge ZVS Converter," IEEE Transactions on Power Electronics, Vol. 19, No. 3, pp. 701-708, May 2004.

[11] Min Chen, Dehong Xu, Mikihiko Matsui, "Study on Magnetizing Inductance of High Frequency Transformer in the Two-Transistor Forward Converter," Power Conversion Conference 2002, Vol. 2, pp. 597-602, 2002.

[12] Dharmraj V. Ghodke, K. Muralirishnan, "1.5kW two switch forward ZCZVS converter using primary side clamping," Power Electronics Specialists Conference 2002, Vol. 2, pp. 893-898, 2002.
[13] F.L. Luo, H. Ye, "Positive output cascade boost converters," IEE Proceedings, Electric Power Applications, Vol. 151, No. 5, pp. 590-606, Sept. 2004.
[14] J. Leyva-Ramos, M.G. Ortiz-Lopez, L.H. Diaz-Saldierna, M. Martinez-Cruz, "Average current controlled switching regulators with cascade boost converters," IET, Power Electronics, Vol. 4, No. 1, pp. 1-10, Jan. 2011.
[15] H.Y. Kanaan and G. Sauriol, K. Al-Haddad "Small-signal modeling and linear control of a high efficiency dual boost single-phase power factor correction circuit," IET Power Electrons, Vol. 2, No. 6, pp. 665-674, Nov. 2009.

Yun-Sung Kim He received his B.S. and M.S. degrees in Electrical Engineering from Cheongju University, Cheongju, Korea, in 2000 and 2002. He joined the Research & Development Center at Dongahelecomm Corporation, Yongin, Korea, in 2002 where he has worked for Advanced Development Team in R&D Center as a senior engineer since 2004. And he has worked for his Ph.D. in Electrical Engineering at Sungkyunwan University, Suwon, Korea, since 2010. His research interests include battery charger for PHEV/EV, renewable energy conversion system, bi-directional power conversion device, and high efficiency resonant converters.

Dong-Wook Jung He received his B.S. degrees in Electrical Engineering from Myongji University, Yongin, Korea, in 2010. He joined Advanced Development Team at Dongahelecomm Corporation, Yongin, Korea, since 2009. His research interests include DC-DC Converters for Telecom, renewable energy conversion system, and high efficiency resonant converters.

Byoung-Kuk Lee He received the B.S. and the M.S. degrees from Hanyang University, Seoul, Korea, in 1994 and 1996, respectively and the Ph.D. degree from Texas A&M University, College Station, TX, in 2001, all in electrical engineering. From 2003 to 2005, he has been a Senior Researcher at Power Electronics Group, Korea Electrotechnology Research Institute (KERI), Changwon, Korea. From 2006 Dr. Lee joins at School of Information and Communication Engineering, Sungkyunkwan University, Suwon, Korea. His research interests include charger for electric vehicles, hybrid renewable energy systems, dc distribution systems for home appliances, power conditioning systems for fuel cells and photovoltaic, modeling and simulation, and power electronics. Prof. Lee is a recipient of Outstanding Scientists of the 21st Century from IBC and listed on 2008 Ed. of Who's Who in America. Prof. Lee is an Associate Editor in the IEEE Transactions on Industrial Electronics and General Chair for IEEE Vehicular Power and Propulsion Conference (VPPC) in 2012.